Research Article

Forecasting the track and intensity Damrey storm in 2017 by the multi–physical ensemble Kalman filter

Minh Thi Pham[1*], Trung Le Doan[2], Hang Thi Nguyen[3], Tuong Hong Thi Tran[4], Thuy Kim Pham[3]

[1] Department of Meteorology, Hydrology and Climate change, Ho Chi Minh University of Natural Resources and Environment; minhpt201@gmail.com
[2] Student of Department of Meteorology, Hydrology and Climate change, Ho Chi Minh University of Natural Resources and Environment; dltrungphuhoi@gmail.com
[3] Department of General Science Ho Chi Minh University of Natural Resources and Environment; hang.nguyen687@gmail.com; pkthuy.math@gmail.com
[4] Department of Information Systems and Remote Sensing, Ho Chi Minh University of Natural Resources and Environment; tthtuong@hcmunre.edu.vn

*Corresponding author: minhpt201@gmail.com; Tel.: +84–936069249
Received: 8 April 2022; Accepted: 22 June 2022; Published: 25 June 2022

Abstract: This study applicates the multi–physical method in ensemble Kalman filter determining error of WRF models to forecast the track and intensity of storm Damrey in 2017. The study run three experiments with assimilation of satellite data to forecast Damrey in 2017 at the beginning 00 UTC and 12 UTC November 1st and 2nd: (1) 21 ensemble members which are combined from 11 physics options, no increase in error correlation (MP); (2) Using single set of physical model, 21 ensemble members, inflation factor $\lambda = 6.5$ (MI); (3) Using single set of physical model, 21 ensemble members without increase in error correlation (PF). Statistical results of track errors in MP test at the 24, 48, 72–hour is 12–32% reduction in compared with tests MI and PF. For storm intensity, absolute error of P_{min} in the MP test at 24 and 72–hour is decreased from 30–47% in compared to the other two tests. And the absolute error of Vmax in the MP test at all forecasting terms is 13–26% reduction in compared with tests MI and PF. Thus, the multi–physical ensemble Kalman filter can forecast the track and intensity of storms affecting Vietnam.

Keywords: Ensemble forecasting; Error model; Typhoon; The Kalman filter.

_____

1. Introduction

Basically, data assimilation is a process which the observed data and a background guess field are statistically combined to obtain the best possible initial conditions for the numerical model [1–2]. The goal of assimilation is to find the best possible analysis field for the model input. However, this work depends heavily on the quality of the observed data (related to the error of the observed data) and the quality of the model's background guess data (related to the model's intrinsic error). The error related to the monitoring data belongs to the problem of quality control of professional monitoring; while the background field error is related to the model's internal errors – errors caused mainly by physical processes that are not fully understood [2–4].

Currently, the model error handling techniques in modern data assimilation algorithms include multiplicative inflation techniques [5], additive increasing techniques [6], or

systematic error correction method [7–8], multiple physics technique [9]. The multiple physics technique is the method of using different combinations of physical parameterization diagrams in the WRF model to calculate the parameters related to the error of the model in the ensemble Kalman filter [9]. This method is based on the assumption that the source of the model error is mainly due to the incomplete representation of physical processes [2–3]. The multiple physics has been applied in some previous studies [3, 9–11], and show significant improvements in track and intensity storm prediction results compared with other methods, such as the multiplicative inflation [12] and compared with the case where the model error is zero [3, 9–11]. Accordingly, in the study [9], it was shown that the multiplicative inflation factor 6.5 is the best compared to the multiplicative inflation factor that varies from 1.0 to 6.5, and the multiple physics technique is good choice for short–term forecasting problem, in addition, the study also shows that the optimal number of combinations in combination prediction ranges from 21–24 components which are different combinations of physical parameterization schemes in the WRF model. Therefore, in this study, we will use the multiplicative inflation technique and consider the model to be perfect to compare with the multiple physics' technique, and the number of ensemble components is 21 components for a forecasting session [9].

In addition, storm Damrey in 2017 was a strong storm that directly hit Ninh Hoa–Khanh Hoa At 6:30 am on 4 November 2017 with wind strength increased by 1 level to level 13, level 15, 16 [13]. At 10 o'clock on the same day, the center of the storm was on the mainland of Dak Lak–Lam Dong, the wind strength near the center of the storm decreased to level 10–11, level 13. After that, the storm weakened into a tropical depression. By noon on November 5, the center of the tropical depression in the southern region of Cambodia, the wind dropped below 40 km/h. By November 8, at least 106 people had been killed in Vietnam by the storm, with 197 others injured and 25 missing. It is reported that more than 116,000 homes were destroyed after flooded. The United Nations Children's Fund (UNICEF) estimates that at least four million people have been directly impacted by the storm and need support. Nha Trang beach resort was one of the hardest hit areas, 30,000 residents and tourists had to evacuate the area. A number of previous studies used storm Damrey as in the initial study of vortex chemistry by Nguyen Binh Phong and Associates 2020 to predict the intensity of storm Damrey during the landfall stage [14]. Research results show that storm intensity with vortex initial is improved more clearly in the absence of vortex initialization. Another study related to the forecast of the storm Damrey's trajectory by the method of correcting the forecast of the storm's trajectory from the product of the combined forecasting system through the selection of the optimal composite component of the author Tran Quang Nang and Tran Tan Tien 2020 [15]. The results show that the correction method can only improve the error of trajectory prediction in short–term forecasting terms. Another study by Kulaya Keawsang–in and colleagues 2021 examines the sensitivity of different physical schemes to simulate Typhoon Damrey. The results show that the Belts–Millers–Janjic convection diagram and the WSM6 microphysics diagrams are suitable in the simulation of storm Damrey [16]. Therefore, in this study, we apply multiphysics technique in combinatorial Kalman filter to determine the error of WRF model predicting the trajectory and intensity of storm Damrey 2017.

2. Methods and data

2.1. Ensemble Kalman Filter algorithm

The idea of the LETKF algorithm is to use the background ensemble matrix as a transformation operator from the model space spanned by the grid points within a selected local patch to the ensemble space spanned by the ensemble members, and perform the analysis in this ensemble space at each grid point. For a quick summary of the LETKF

algorithm, assume that a background ensemble $\{\mathbf{x}^{b(i)} i = 1, 2..., k\}$ are given, where k is the number of ensemble members (assuming that we are doing analysis at one instant of time, so no time index is written explicitly). Following [17], an ensemble means $\bar{\mathbf{x}}^b$ and an ensemble perturbation matrix $\mathbf{X}^b$ are defined respectively as:

$$\bar{\mathbf{x}}^b = \frac{1}{k}\sum_{i=1}^{k}\mathbf{x}^{b(i)} \; ; \; \mathbf{X}^b = \mathbf{x}^{b(i)} - \bar{\mathbf{x}}^b \tag{1}$$

Let $\mathbf{x} = \bar{\mathbf{x}}^b + \mathbf{X}^b\mathbf{w}$, where $\mathbf{w}$ is a local vector in the ensemble space, the local cost function to be minimized in the ensemble space is given by:

$$\widehat{J}(\mathbf{w}) = (k-1)\mathbf{w}^T\{\mathbf{I} - (\mathbf{X}^b)^T[\mathbf{X}^b(\mathbf{X}^b)^T]^{-1}\mathbf{X}^b\}\mathbf{w} + J[\mathbf{x}^b + \mathbf{X}^b\mathbf{w}] \tag{2}$$

where $J[\mathbf{x}^b + \mathbf{X}^b\mathbf{w}]$ is the cost function in the model space. If one defines the null space of $\mathbf{X}^b$ as N = $\{\mathbf{v} \mid \mathbf{X}^b\mathbf{v} = 0\}$, then it is easy to see that the cost function $\widehat{J}(\mathbf{w})$ is composed of two parts: one containing the component of $\mathbf{w}$ in N (the first term in Eq. 2), and the second depending on the component of $\mathbf{w}$ that is orthogonal to N. By requiring that the mean analysis state $\bar{\mathbf{w}}^a$ is orthogonal to N such that the cost function $\widehat{J}(\mathbf{w})$ is minimized, the mean analysis state and its corresponding analysis error covariance matrix in the ensemble space can be found as:

$$\bar{\mathbf{w}}^a = \widehat{\mathbf{P}}^a(\mathbf{Y}^b)^T\mathbf{R}^{-1}[\mathbf{y}^0 - H(\bar{\mathbf{x}}^b)] \tag{3}$$

$$\widehat{\mathbf{P}}^a = [(k-1)\mathbf{I} + (\mathbf{Y}^b)^T\mathbf{R}^{-1}\mathbf{Y}^b]^{-1} \tag{4}$$

where $\mathbf{Y}^b \equiv H(\mathbf{x}^{b(i)} - \bar{\mathbf{x}}^b)$ is the ensemble matrix of background perturbations valid at the observation locations, and $\mathbf{R}$ is the observational error covariance matrix. By noting that the analysis error covariance matrix $\mathbf{P}^a$ in the model space and $\widehat{\mathbf{P}}^a$ in the ensemble space have a simple connection of $\mathbf{P}^a = \mathbf{X}^b\widehat{\mathbf{P}}^a(\mathbf{X}^b)^T$, the analysis ensemble perturbation matrix $\mathbf{X}^a$ can be chosen as follows:

$$\mathbf{X}^a = \mathbf{X}^b[(k-1)\widehat{\mathbf{P}}^a]^{1/2} \tag{5}$$

The analysis ensemble $\mathbf{x}^a$ is finally obtained as:

$$\mathbf{x}^{a(i)} = \bar{\mathbf{x}}^b + \mathbf{X}^b\{\bar{\mathbf{w}}^a + [(k-1)\widehat{\mathbf{P}}^a]^{1/2}\} \tag{6}$$

Detailed handling of more general nonlinear and synchronous observations in LETKF can be found in [17]. It should be mentioned that the above formation is only valid in the absence of model errors. To take into account the model errors, [17] suggested that a multiplicative factor should be introduced in Eq. (4) (specifically, the first factor on the rhs bracket in Eq. 4). Although one could also use the additive inflation, this study focuses only on the multiplicative inflation for the ease of implementation and comparison.

2.2. Models and Study area

Using WRF model version V3.9.1 with 31 levels (Sigma) in the vertical with the highest-pressure level (the upper boundary of the model) is 10hPa [18]. The WRF model is selected with two nested computational domains using the Mercator projection. The mesh area designed for the simulation test of Damrey storm is a nested grid consisting of 2 regions with horizontal resolutions of 36 km and 12 km respectively, grid domain 1 consists of 151×151 grid points and grid domain 2 consists of 151×151 grid points with the domain center. immobility 11.2°N & 112.3°E (Figure 2).
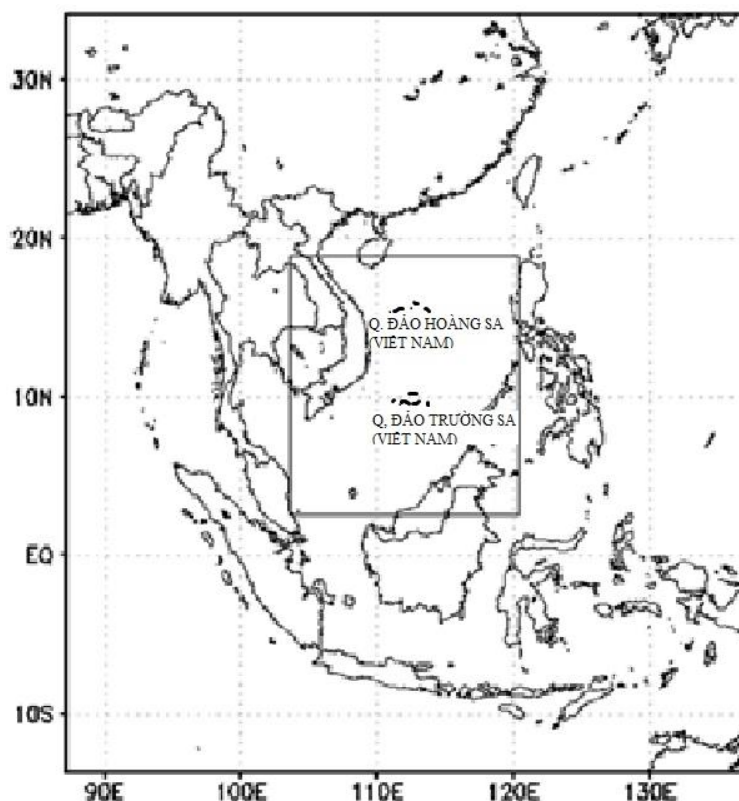
Figure 1. The study area.

2.2. Experiment descriptions

In this study, the authors tested the forecast for typhoon Damrey 2017 with a term of 3 days 2017 at the beginning 00 UTC and 12 UTC November 1st and 2nd with experiments are listed in table 1. All the above tests are assimilated satellite wind data by the ensemble Kalman filter.

Table 1. List of experiments with the WRF–LETKF configuration.

Experiments	Description	Boundary Condition
MP	The Combination of 11 options physical model, 21 ensemble members, no increase in error correlation	To ensure that each member has its own lateral boundary condition consistent with its updated nalysis,
MI	Using a set of physical model, 21 ensemble members, inflation factor λ = 6.5	the WRFDA boundary routine is used to generate boundaries for each
PF	Using a set of physical model, 21 ensemble members without increase in error correlation	ensemble member after the ensemble analysis step is finished for every cycle.

In the first experiment (MP), 21 sets of physical models (Table 3) consisted of the set of combinatorial components of the parameterization schemes in Table 2. In the second experiment (MI), one the set of specific physical models in the WRF model include (a) the WSM3 microphysics diagram, (b) the radiation rapid transmission scheme (RRTM) for both long and short-wave radiation, and (c) BMJ convective parameterization scheme (component 11) is applied to all combinatorial components with a multiplier = 6.5 added in the variable error correlation matrix change P^a in expression (4). However, this coefficient λ does not change in all cycles of the experiment so that the effectiveness of the MI method in handling model error can be compared with that of the MP method. In the third experiment (PF), we consider the model to be perfect with the background error unchanged over all the running cycles of the experiment. Similar to the multiplication method, this

experiment uses the same set of physical models as in the MI experiment so that the effectiveness of the method in handling model errors can be compared with the MP and MI tests.

Table 2. Options table of physical parameterization schemes in WRF model [19].

Schemes	Symbol	Options
Longwave Radiation	**ra_lw_physics**	1. RRTM scheme
Shortwave Radiation	**ra_sw_physics**	1. Dudhia scheme 2. Goddard shortwave
Microphysics	**mp_physics**	1. Kessler scheme 2. Lin et al. scheme 3. WSM 3–class simple ice scheme 4. WSM 5–class scheme 5. Ferrier (new Eta) microphysics 6. WSM 6–class graupel scheme
Cumulus Parameterization	**cu_physics**	1. Kain–Fritsh scheme 2. Betts–Miller–Janjic scheme

Table 3. Encryption of multi–physical ensembles from multiple physics options in WRF model [19].

Complex	Ra_lw_ physics	Ra_sw_ physics	mp_ physics	cu_physics
001	1	2	1	1
002	1	1	1	2
003	1	2	1	2
004	1	1	2	1
005	1	2	2	1
006	1	1	2	2
007	1	2	2	2
008	1	1	3	1
009	1	2	3	1
010	1	1	3	2
011	1	2	3	2
012	1	1	4	1
013	1	2	4	1
014	1	1	4	2
015	1	2	4	2
016	1	1	5	1
017	1	2	5	1
018	1	1	5	2
019	1	2	5	2
020	1	1	6	1
021	1	2	6	1

2.3. Data

The initial and boundary conditions used NCEP/NCAR (NCEP–The National Center for Environmental Prediction/NCAR–The National Center for Atmospheric Research) GFS forecast data with a horizontal resolution of 0.5×0.5 degrees and grib2 format. GFS data were obtained from the website: https://www.ncdc.noaa.gov/data-access/model-data/model-datasets/global-forcast-system-gfs. The best track data of storm position and intensity are collected from the website: https://www.metoc.navy.mil/jtwc/jtwc.html?western-pacific.

Wind monitoring data from satellites is a particularly important data source for forecasting models running around the world with global coverage and data collection time within 3–6 hours. depending on the characteristics of each satellite. Satellite wind data allows to know the dynamic state of the atmosphere, contributing to the information of the initial field of the forecast model by data assimilation. Currently, satellite wind data are

preprocessed by the University of Wisconsin satellite atmospheric motion vector CIMSS–AMV (Cooperative Institute for Meteorological Satellite Studies – University of Wisconsin satellite atmospheric motion vector CIMSS–AMV) in the same time period. selected. Several studies with CIMSS–AMV data have shown that this data can help improve the predictive quality of various medium–sized systems. The advantage of the CIMSS–AMV data is that the error has been tested for high quality and is determined by a recursive filtering algorithm. Each metric is checked for the best fit with the surrounding data using quality index techniques. Most of the CIMSS–AMV data is distributed in different regions and is currently stored in a variety of formats including ASCII and/or BUFR. In this study, satellite wind data were collected over the Indian, Northwest Pacific region (Figure 2) and downloaded from the website http://tropic.ssec.wisc.edu in ASCII format.
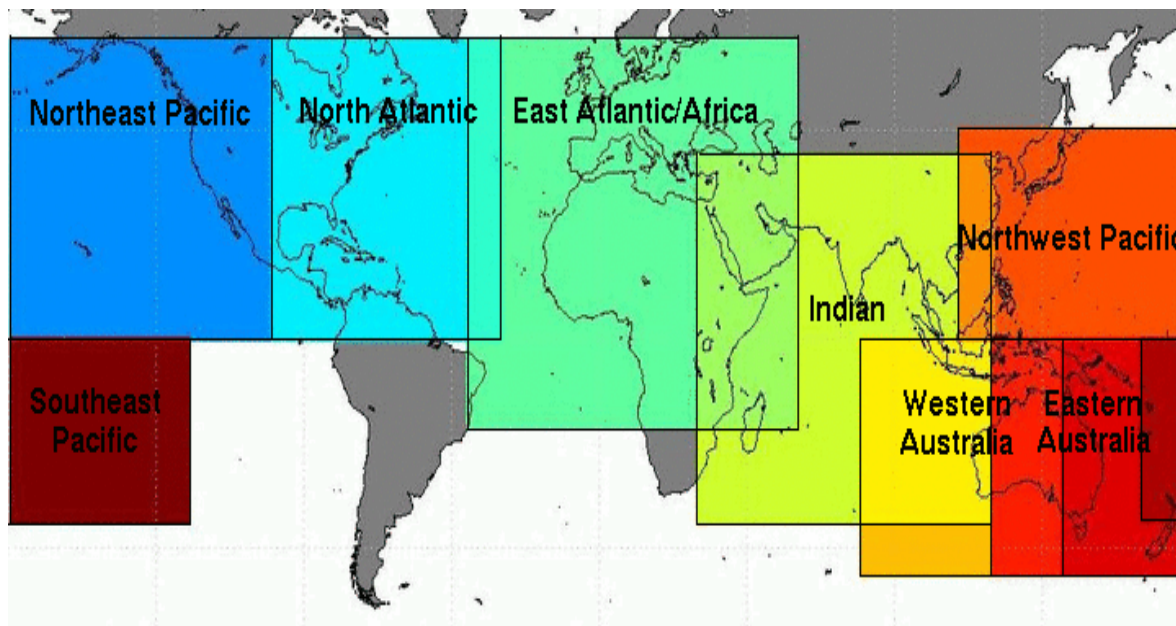

Figure 2. Area is covered by satellite wind data in this study (source: http://tropic.ssec.wisc.edu).

2.4. Evaluation methods

2.4.1. Absolute mean method

According to [20], MAE error is used to evaluate the predictions of continuous atmospheric variables. Therefore, MAE is applied as an index to evaluate the error of storm intensity (minimum sea level pressure at the center – PMIN and maximum wind speed near the center of VMAX). With MAE–mean absolute error is calculated by the formula:

$$\text{MAE} = \frac{1}{N}\sum_{i=1}^{N}|F_i - O_i| \qquad (7)$$

where MAE is the mean absolute error; F_i is the predicted value; O_i is the observed value; and N is the length of the data series.

2.4.1. Storm center distance method

Track error calculated by formula (8).

$$\text{PE} = R_e * \arccos\left[\sin(\alpha_1) * \sin(\alpha_2) + \cos(\alpha_1) * \cos(\alpha_{2)} * \cos(\beta_1 - \beta_2)\right] \quad (8)$$

where R_e is the radius of the earth (6378.16 km); α_1, α_2 is the latitude of the actual of the storm and the center of the storm predicted by the model (in radians); β_1, β_2 is the longitude of the actual center of the storm and the predicted center of the storm (in radians). The distance mean error is calculated as follows:

$$MPE_j = \frac{\sum_{i=1}^{n} PE_{i,j}}{n} \tag{9}$$

where PE is the distance error of each forecasting case; n is the number of test cases; j is the forecast term.

3. Results and discursion

3.1. Stream simulation

Basically, when large–scale circulations change and control the storm's active area, it will directly affect the direction of the storm's movement. In the case of cyclone Damrey, large–scale circulation dominated the storm's area of activity, including the northwest Pacific subtropical high and cold high at north of the storm. For the purpose of investigating the applicability of multiphysics techniques in determining the model error in ensemble Kalman filter to prediction storm trajectory, the study compares the stream field in the MP, MI and PF tests in levels 850, 700, and 500 hPa at 12h00 UTC on 3rd November 2017 is the time when the storm begins to make landfall in the forecast session that begins at 12h00 UTC on 1st November 2017 (Figure 3).
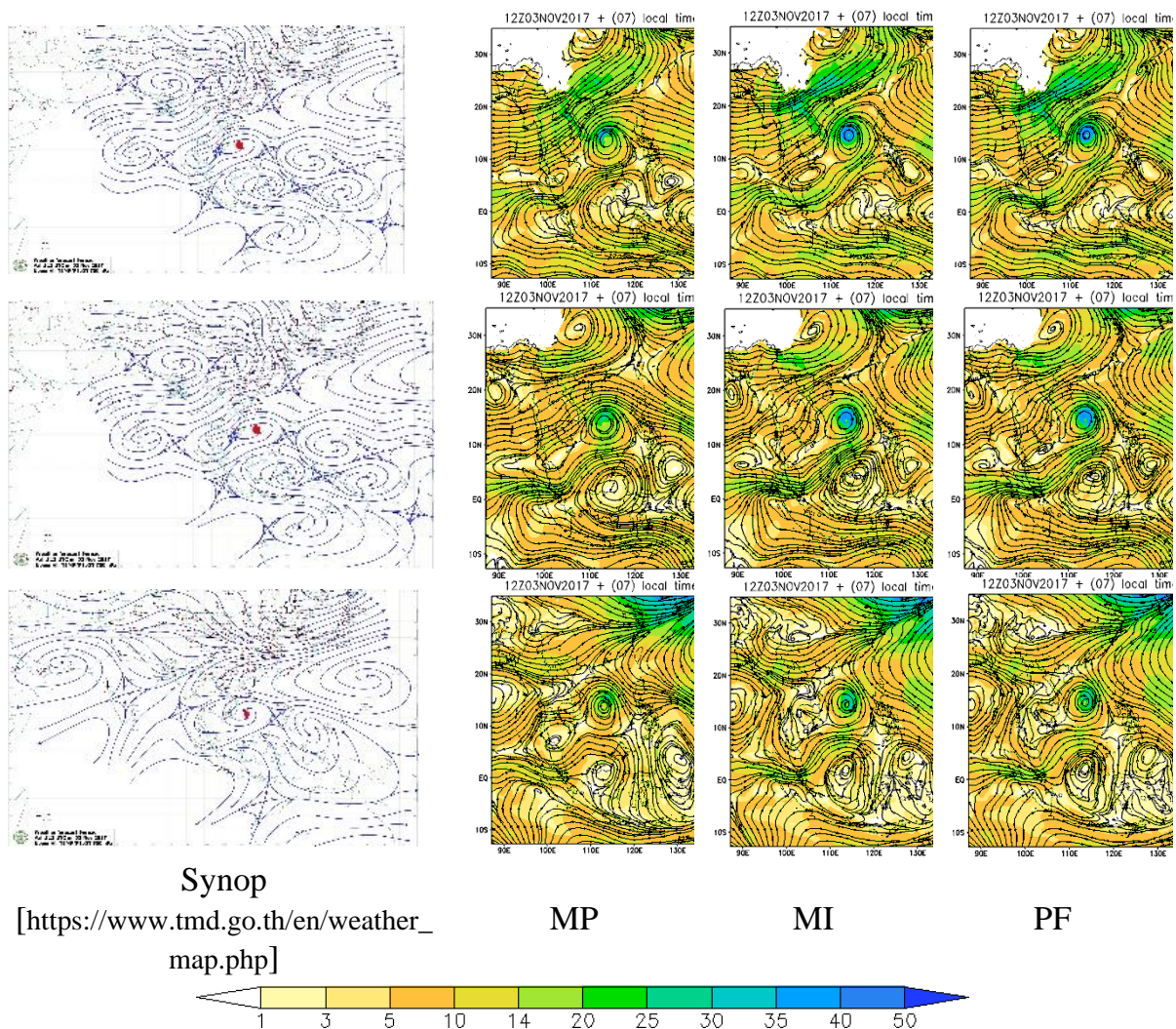

Synop
[https://www.tmd.go.th/en/weather_map.php]   MP   MI   PF

Figure 3. The stream map of 850 hPa (top), 700 hPa (middle) and 500 (bottom) hPa levels.

At 850 hPa and 700 hPa, the MP test simulates a cold high that mixes southward and extends to the east more than the cold high which is simulated in the MI and PF tests. In particular, at 700 hPa and north of the storm there is a fairly barometric saddle in the synop map, and this barometric saddle is also simulated in the MP test, while the MI and PF tests

don't simulate this barometric saddle (Figure 3). At 500 hPa, the MP test simulates the northwest Pacific subtropical high more westward than the MI and PF trials, and has a similar morphology to the synop map (Figure 3). The simulation results show that the direction of the storm in the MP test is closer to the real trajectory than the other two tests [11].

Thus, the multiphysics technique seems to have some impact in the flowline simulation at the levels of 850, 700 and 500 hPa. This result is a consequence of previous work that demonstrated that the volumetric least squares error of the multiphysics technique is smaller than the volumetric least squares error of the multiplicative inflation technique. Meaning predicted error of U, V and T in the MP test improved markedly compared with the MI test [9]. As a result, the forecast results of the trajectory and intensity of storm Damrey in the MP test are also improved relative to the MI and PF tests. In the next section, the paper will examine the ability of the tests to predict the trajectory and intensity of storms.

3.2. *Forecasting intensity and track*

3.2.1. Track storm

Figure 4 shows that the true trajectory of Typhoon Damrey is moving to the west (Figure 4) and made landfall around 12h00 UTC on 3rd November 2017. Meanwhile, the ensemble components in the MP, MI and PF tests all predict the trajectory of storm Damrey to move to the northwest. At 12h00 UTC on 4th November 2017, the storm moved on the sea in MP, MI and PF tests (Figures 4a–4c). In addition, a few ensemble components of the MP test predicted the location of the storm Damrey's landfall, but it is quite far from the actual location. On the other hand, the dispersion of composite components in the MP test is wider than that of the composite components in the MI and PF tests. This result is similar to the results of the previous study when concluding that the composite dispersion in MP was wider than the composite dispersion in the MI test [9, 11].

Figure 4d is the ensemble mean trajectory in the MP, MI and PF tests, the observed trajectory in black and the trajectory of the GFS data (green). From 00–hour to 30–hour forecast period, it shows that the storm trajectory is not much different between the 3 tests MP, MI and PF, after the 30–hour forecast period to 72 hours, the forecast trajectory of the tests is in the north of the true trajectory, where the predicted trajectory of the MP test is closer to the true orbit than the MI and PF tests. And the Damrey orbit in the GFS data is located south of the true trajectory.

The forecast results of storm Damrey's trajectory in the tests are consistent with the results of the stream simulations in all three tests (section 3.1). Specifically at 12h00 UTC on 3 November 2017 At 850 hPa and 700 hPa, the MP test simulates a cold high which moves down to the south and extends to the east more than with cold high simulated in the MI and PF tests. So the cold high in the MP test limited the direction of the storm's movement to the north. In addition, at 500 hPa, the MP test also simulated the northwest Pacific subtropical high developing to the west, thereby also limiting the northward movement of the storm (figure 4d). However, the speed of storm movement in all 3 trials was slower than observed and GFS data. And to quantify the accuracy of each trial's hurricane trajectory prediction, the study calculated the trajectory prediction error of the trials.

From the graph showing the trajectory prediction error of the MP, MI and PF tests together with the trajectory prediction error of the GFS data (Figure 5), it shows that the trajectory prediction error of the MP test is lower than the forecast error of the storm trajectory of the MI and PF tests at most forecasting periods. Meanwhile, the forecast error of storm trajectory in the MP test did not improve much compared with the track forecast error of the GFS data. This result is also clearly seen in the statistics of the orbital forecast error of the 3 forecasting sessions (Figure 6).

To evaluate the effectiveness of the MP test in predicting the trajectory, we calculated the relative trajectory prediction error between the MI and MP tests, and between the PF and MP tests (table 4). The relative trajectory prediction error results show that the orbital error in the MP test improves from 9% to 32% compared to the trajectory prediction error in the MI test, and improves from 4% to 30% compared to the trajectory prediction error in the PF test at most forecasting terms. This result may be due to the multiphysics technique (determining the error of the model due to the incomplete understanding of physical processes [4, 9] has partly corrected the error of the model. So that the received background field has a significantly reduced error, and leads to a more accurate analysis field for the input of the model than the multiplicative inflation technique and considers the model perfect.
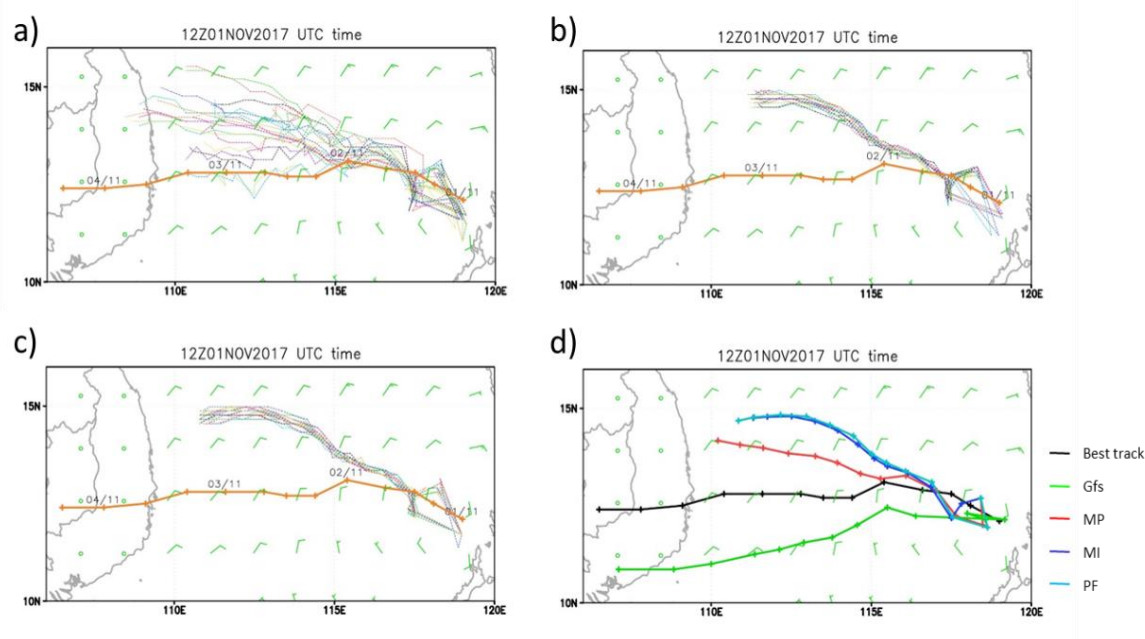

Figure 4. The predicted trajectory of Hurricane Damrey in the MP test (a), the MI test (b) and the PF test (c); observed (orange), composite components are thin lines; Figure d is the observed trajectory, the combined average trajectory of the test MP, MI, PF and GFS data. The forecast start time is 12 o'clock on November 1, 2017.
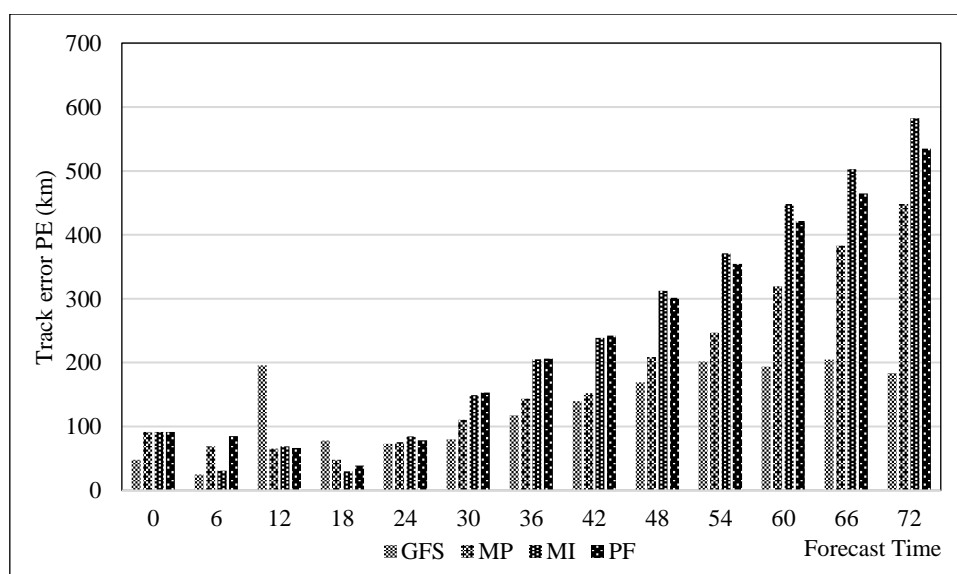

Figure 5. The ensemble means track errors in the MP, MI and PF test. With the forecast session starting at 12h00 UTC on 1st November 2017.
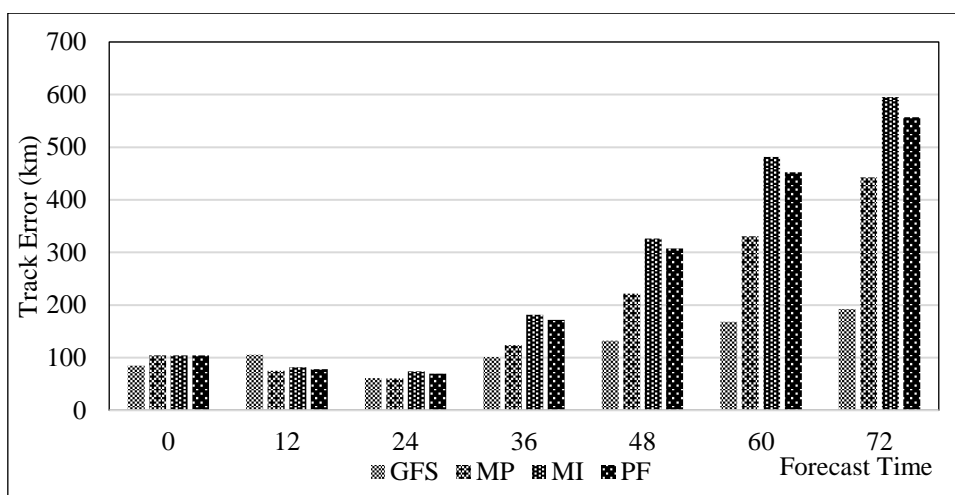
Figure 6. Average track error of 3 forecasting sessions (00 UTC on 1 st November 2017, 12UTC on 1st November 2017 and 00 UTC on 2 nd November 2017) MP, MI, PF test and GFS data.

Table 4. Relative error of MI and PF relative to MP in trajectory simulation, P_{min} and V_{max}.

Periods	Track (km)		Pmin (hPa)		Vmax (ms⁻¹)	
	MI–MP	**PF–MP**	**MI–MP**	**PF–MP**	**MI–MP**	**PF–MP**
0	0.00	0.00	0.00	0.00	0.00	0.00
6	–0.23	0.05	0.08	0.03	–0.03	0.14
12	0.08	0.04	0.08	0.10	–0.03	0.08
18	0.09	0.12	–0.13	–0.19	–0.06	–0.13
24	0.18	0.13	0.31	0.27	0.13	0.18
30	0.32	0.28	–0.30	–0.32	0.49	0.49
36	0.32	0.28	–0.16	–0.17	0.36	0.35
42	0.32	0.28	0.68	0.62	0.58	0.52
48	0.32	0.28	–1.56	–1.32	0.27	0.18
54	0.34	0.30	–0.05	–0.05	0.07	0.08
60	0.31	0.27	0.25	0.18	0.30	0.29
66	0.31	0.26	0.38	0.35	0.24	0.19
72	0.26	0.21	0.47	0.43	0.26	0.21

3.2.2. Damrey storm intensity

Storm intensity is usually expressed through minimum pressure (P_{min}) and maximum wind speed (V_{max}). The P_{min} and V_{max} values used in this section are the mean of the 21 ensemble members in each trial.

a) The minimum pressure

The observed P_{min} data in Figure 7 shows that the storm gradually became stronger from 12h00 UTC on 1st November 2017 and the strongest storm at 12h00 UTC on 3rd November 2017 (Figure 7) – expressed through the value of P_{min} down to the lowest. After that, the P_{min} value increases gradually, meaning the storm is getting weaker. The MP, MI and PF tests all predict the P_{min} process which has a decreasing trend similar to the observed P_{min} value. However, after 12h00 UTC on 3rd November 2017, these tests did not predict the changing trend of the P_{min} process as observed (Figure 7). Particularly, the P_{min} of GFS data has a variable similar to the observed P_{min}, but value P_{min} is much larger than the observed P_{min} value, or in other words, the storm intensity in the GFS data is weaker than in reality. At 12h00 on 3rd November 2017 is also the time when the storm makes landfall (according to monitoring data), but in the tests, P_{min} decreased little or not, so the storm still existed at sea. This result is statistically consistent, when the storm makes

landfall, the intensity of the storm decreases. Meaning the P_{min} value increases more than on the sea surface.

The P_{min} absolute error results will indicate the effectiveness of each trial in predicting P_{min}. Figure 8 shows that the P_{min} absolute error in the MP test did not improve much compared to the MI and PF tests at the 60–hour advance term, while at the 66–hour and 72–hour forecast period, the MP absolute error improved significantly. Statistically, all 3 forecasting sessions showed that P_{min} prediction results in the MP test were better than the MI and PF tests at most of the forecasting term (Figure 9).

In addition, similar to the evaluation of the predictability of the Damrey storm trajectory of the multiphysics technique in determining the error of the model in the ensemble Kalman filter, we also calculate the relative error P_{min} between the tests. The results in Table 4 show that, at the 24–hour forecast period and the 2–day prediction term, the MP test improves the P_{min} error by 18% to 47% compared with the MI and PF tests. This result may be due to the effect of the multiphysics technique in forecasting meteorological variables (U, V and T) which is significantly improved compared with the techniques in the MI test [9] and PF test. On the other hand, the P_{min} statistical error results also show that the MP test significantly improves the P_{min} error compared with the GFS data (Figure 9) at most of the forecasting term. However, at the time when the storm was about to make landfall, the P_{min} error in the MP test did not improve compared to the initialization vortex method [14]. In the next section, the article analyzes the predictive ability of Vmax of multiphysics techniques.
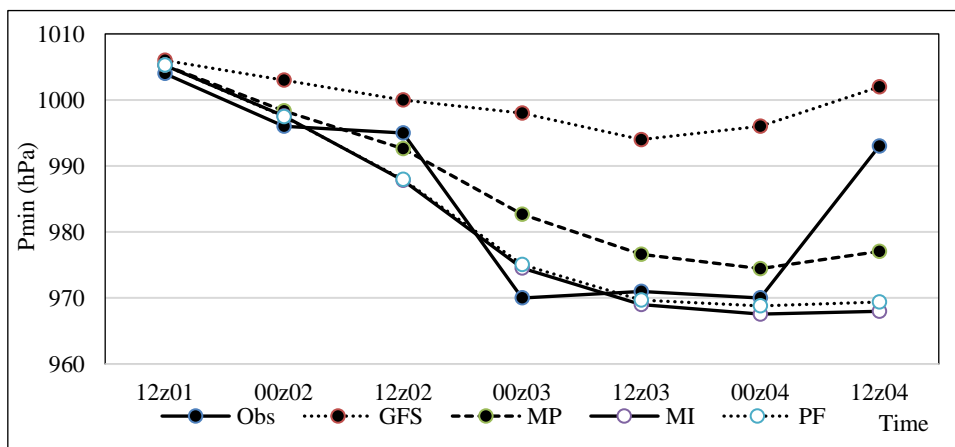

Figure 7. The mean P_{min} process variable in the trials. With the forecast start time at 12h00 UTC on 1st November 2017.
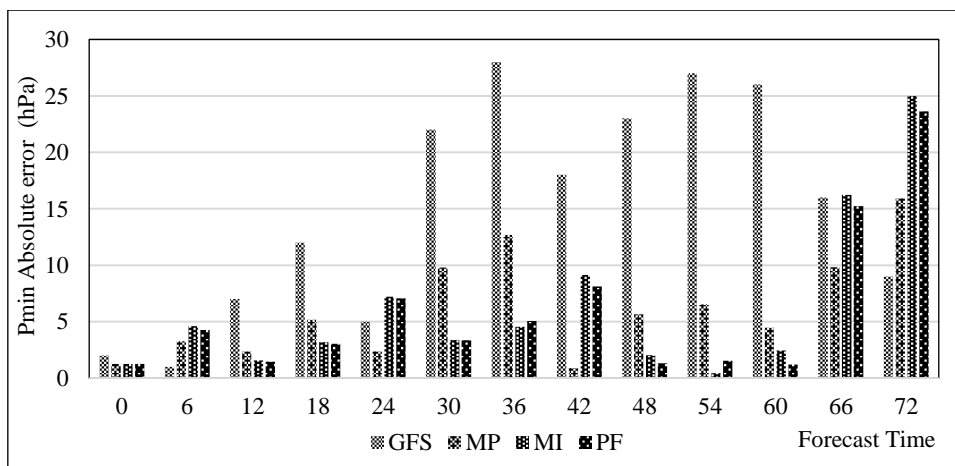

Figure 8. P_{min} Absolute error (hPa) in the MP, MI, PF test and GFS data. Forecast at 12h00 UTC on 1st November 2017.
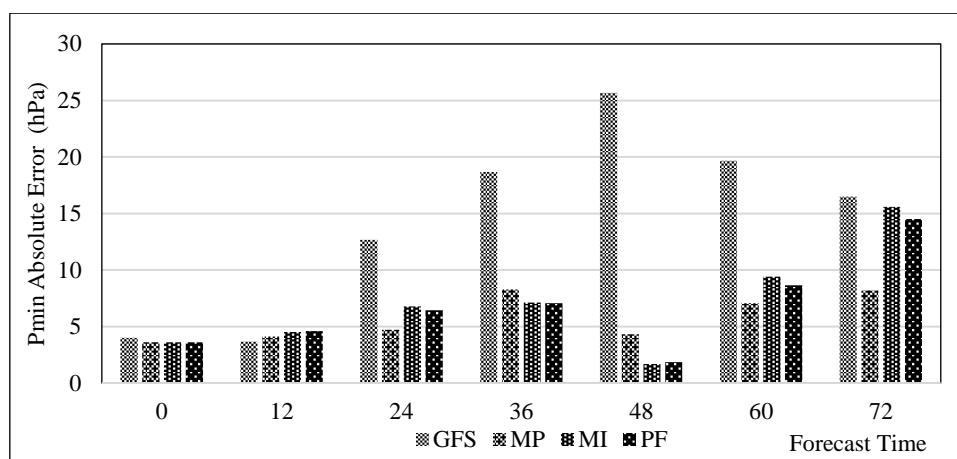
Figure 9. Average absolute error P$_{min}$ in forecast sessions (00 UTC on 11/01/2017, 12 hours UTC on 11/01/2017, 00 UTC on 11/2/2017) in MP, MI, PF tests and GFS data.

b) Maximum wind speed

The maximum wind speed (V$_{max}$) is the second factor representing the intensity of any storm. The change in Vmax during the storm's activity also indicates that the storm is weakening or strengthening. Therefore, the V$_{max}$ variable is a visual image describing the strength or weakening of the storm. Figure 10 is the Vmax variable of storm Damrey with the forecast time at 12h00 UTC on 1st November 2017. Similar to the Pmin variable, the observed Vmax data shows that the storm is getting stronger from 12h00 UTC on 1st November 2017 and the strongest at 12h00 on 3rd November 2017 – this is shown by the value of Vmax reaching the minimum at this time. After that, the storm gradually weakened when it made landfall, due to the influence of surface friction (Figure 8). Meanwhile, the MP, MI and PF tests all predict that the Vmax process tends to increase similarly to the observed Vmax value from 1200h UTC on 1st November 2017 to 12h00 UTC on 3rd November 2017. After 12h00 on 3rd November 2017, the variable Vmax in the tests is different from the observed Vmax variable (Figure 10). Particularly, the Vmax variable of GFS has a variable similar to the observed V$_{max}$, but V$_{max}$ value is much smaller than the observed Vmax value or in other words, the storm intensity in the GFS data is weaker than in reality. This is consistent with previous studies that simulate the Vmax magnitude of GFS data biased lower than reality. In addition, at 12h00 on 3rd November 2017 is also the time when the storm makes landfall (according to observational data – figure 10, figure 4 – trajectory), but in the tests, V$_{max}$ decreased slightly, so the storm still exists at sea. This result is statistically consistent, when the storm makes landfall, the intensity of the storm decreases sharply – the V$_{max}$ value decreases more than on the sea surface. The results of V$_{max}$ absolute error show the effectiveness of each test in predicting V$_{max}$. Figure 11 shows that the Vmax absolute error of the MP test is significantly improved compared with the MI and PF tests at most of the forecasting terms. Statistically, all 3 forecasting sessions showed that V$_{max}$ prediction results in MP test were better than MI and PF tests at most of the forecast periods except for the 24 hours period (Figure 11).

In addition, we calculate the V$_{max}$ relative error betweenthe tests. The results shown in Table 4 show that the Vmax error value in the MP test is improved by 6% to 58% compared tothe Vmax error in the MI and PF test. This result may be due to the effect ofthe multiphysics technique in forecasting meteorological variables (U, V and T) which is significantly improved compared with the techniques in the MI test [9] and PF test. In addition, the statistical Vmax error also showsthat the MP test significantly improves the Vmax error compared with the GFSdata (Figure 12). However, at the time when the storm was about to makelandfall, the V$_{max}$ error in the MP test did not improve compared to theinitialization method [14]. Thus, for intensity forecasting of Damrey storm, multiphysics

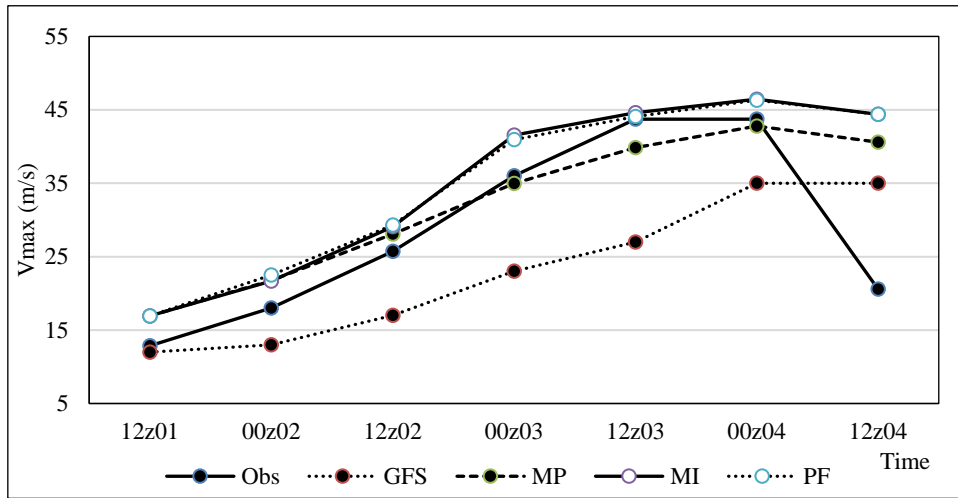techniques show certain advantages – forecasting storm intensityis more effective than other techniques.

Figure 10. Variable V_{max} means in the trials. With forecast start time at 12h00 UTC on 1st November 2017.
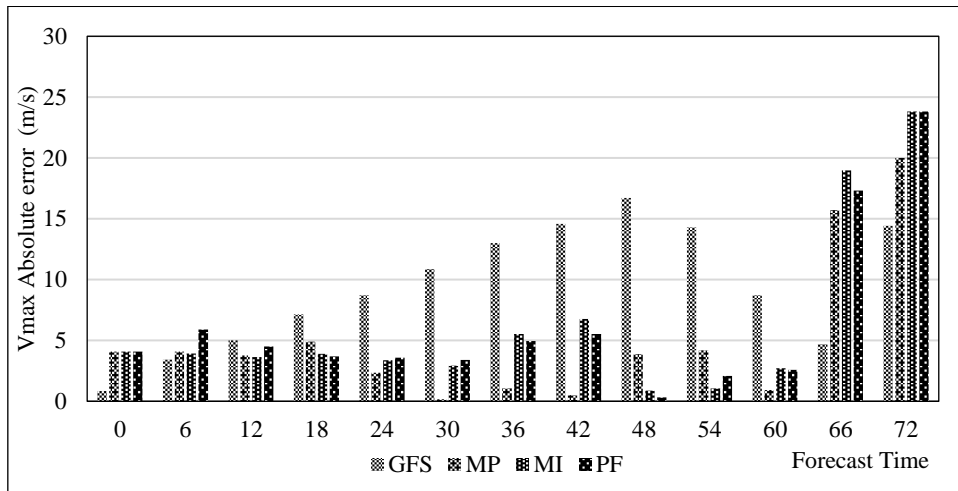

Figure 11. Absolute error V_{max} (m/s) in the MP, MI, PF and GFS tests. Forecast at 12h00 UTC on 1st November 2017.
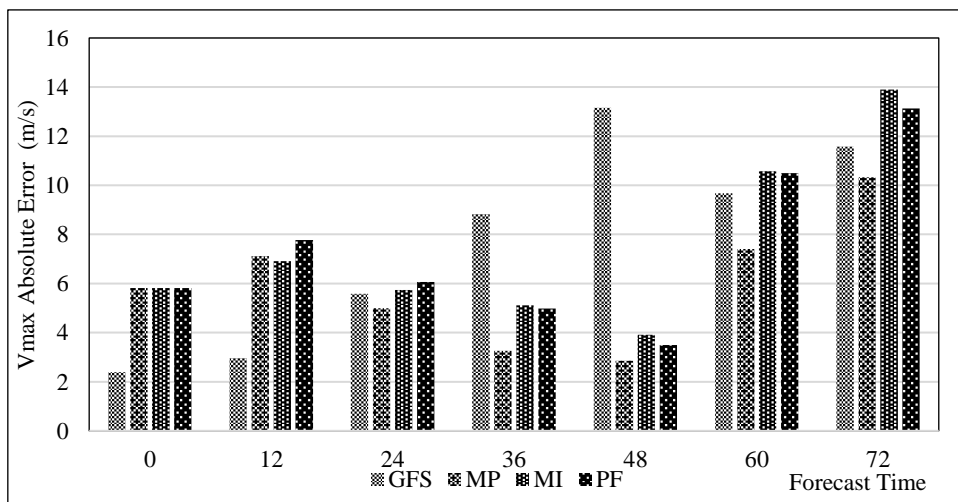

Figure 12. Average absolute error V_{max} in forecasting sessions (00 UTC on 11/01/2017, 12 hours UTC on 11/01/2017, 00 UTC on 11/2/2017) in MP, MI tests, PF and GFS.

4. Conclusion

In this study, we applied multi–body and multiplier technique and considered the model to be perfect to perform 3 sessions of forecasting the trajectory and intensity of Typhoon Damrey 2017 with 3–day forecast period with input field. is the analysis data which is generated from the Kalman filter combination assimilation of wind data observed from satellites. The results of the comparative analysis and comparison between the above methods show that:

Regarding the trajectory prediction, the MP test (multiphysics technique) showed an improved trajectory error of 9% to 32% in compared with the trajectory prediction error in the MI test, and an improvement of 4% up to 30% of the orbital prediction error in the PF test at most forecasting terms. These results are the consequence of correcting the error of the model because the object processes are not fully represented by the multibody technique. With a specific case at the 12h00 session on 1st November 2017, the multi–physical techniques (MP test) simulation results of the general atmospheric circulation – Cold continental high pressure and subtropical high pressure. The north–west Pacific temperature is quite similar to the synaptic topology, so that the forecasted storm trajectory is closer to the true trajectory than the other techniques (MI and PF). However, at the stage when the storm was about to make landfall, the multiphysics technique did not improve the orbital error compared with the GFS data. This may be due to the storm's interaction with land (topography), so the model error at this point does not seem to be simply due to the physical processes in the model not being fully represented enough. Therefore, the study proposes for the next research direction of applying multiphysics technique in combinational Kalman filter to determine model error for simple cases of storms moving at sea and for hurricanes. landed on land. From there, there is a plan to overcome the error of the trajectory for the case of storms that are about to land on the mainland.

In predicting the intensity (P_{min} and V_{max}), the multiphysics technique also shows the certain advantages over the other two techniques at each forecasting term. Specifically, for P_{min}, at the 24-hour forecast period and the 2 days larger forecast period, the MP test improved 18% to 47% of the P_{min} error in compared with the MI and PF tests. For Vmax, the Vmax error value in the MP test improved by 6% to 58% in compared with the Vmax error in the MI and PF test. These results may be due to the effect of the multiphysics technique in predicting meteorological variables (U, V and T) which is significantly improved compared with the multiplier techniques in the MI test [9] and PF. In compared with using GFS data, the multiphysics technique significantly improved the forecast error of storm intensity (Figure 14 and Figure 15). Especially when the storm was about to make landfall, the strongest storm was at 12h00 UTC on 3rd November 2017, the MP test predicted the storm's value as well as the strengthening trend. In terms of errors, P_{min} and V_{max} are improved compared with GFS data, MI and PF tests, but cannot be improved compared to P_{min} and V_{max} prediction results in the initial study of vortex chemistry [14]. Therefore, the research direction that applies both the multiphysics method and the initial application of vortex chemistry to predict the intensity of storms affecting Vietnam is the next research direction of the authors' group.

Author contribution statement: Conceived and designed the experiments; Analyzed and interpreted the data; contributed reagents, materials, analysis tools or data; manuscript editing: M.P.T.; T.D.L.; H.N.T.; T.H.T.T.; T.P.K.; Performed the experiments; contributed reagents, materials, analyzed and interpreted the data, wrote the draft manuscript: M.P.T.; T.D.L.; H.N.T.; T.H.T.T.

References

1. Holton, J.R. An introduction to dynamic meteorology, 2004.

2. Chanh, K.Q. Estimation of Model Error in the Kalman Filter by Perturbed Forcing. *VNU J. Sci.: Nat. Sci. Tehnol.* **2010**, *26(3S)*, 310–316.

3. Thomas, M.H.; Jeffrey, S.W. Accounting for the Error due to Unresolved Scales in Ensemble Data Assimilation: A Comparison of Different Approaches. *Mon. Weather Rev.* **2005**, *133*, 3132–3147.

4. Pu, Z. Improving Hurricane Intensity Forecasting through Data Assimilation: Environmental Conditions Versus the Vortex Initialization, Recent Hurricane Research – Climate, Dynamics, and Societal Impacts. Anthony Lupo (Ed.), **2011,** ISBN: 978-953-307-238-8.

5. Anderson, J.L.; Anderson, S.L. A Monte Carlo implementation of the non–linear filtering problem to produce ensemble assimilations and forecasts. *Mon. Wea. Rev.* **1999**, *127*, 27–41.

6. Mitchell, H.L.; Houtekamer, P.L. An adaptive ensemble Kalman filter. *Mon. Wea. Rev.* **2000**, *128*, 416.

7. Dee, D.P.; Silva, A.M. Data assimilation in the presence of forecast bias. *Quart. J. Roy. Meteor. Soc.* **1998**, *124*, 269.

8. Li, H. Local ensemble transform Kalman filter with realistic observations. Ph.D. dissertation. University of Maryland. 2007, pp. 131.

9. Chanh, K.; Minh, P.T.; Mai, H.T. An Application of the Multi–Physics Ensemble Kalman Filter to Typhoon Forecast. *Pure Appl. Geophys.* **2013**, *170*, 745–954.

10. Jun, L.I.; Jun, D.U.; Yu, L.I.U. A comparison of initial condition-, multi-physics- and stochastic physics-based ensembles in predicting Beijing "7.21" excessive storm rain event. *Acta Meteorol. Sinica* **2014**. doi:10.11676/qxxb2015.008.

11. Minh, P.T.; Hang, N.T.; Thuy, P.K.; Gia, C.N.H. An application of the multi-physical method of determining error of WRF models to simulate the track and intensity Usagi storm in 2018. *Sci Technol. Dev. J.: Sci. Earth Environ.* **2021**, *5(1)*, 298–311.

12. Anderson, J.L.; Anderson, S.L. A Monte Carlo implementation of the non–linear filtering problem to produce ensemble assimilations and forecasts. *Mon. Wea. Rev.* **1999**, *127*, 2741–2758.

13. https://en.wikipedia.org/wiki/Typhoon_Damrey_(2017).

14. Phong, N.B.; Hiep, N.V.; Thang, N.V. Application of dynamical vortex initialization scheme on intensity forecast and structure study of typhoon Damrey (2017) during near-shore and landfalling period. *J. Clim. Change Sci.* **2020**, *16,* 23–35.

15. Nang, T.Q.; Tien, T.T. Skill validation of probability tropical cyclone track forecast in Bien Dong. *VN J. Hydrometeorol.* **2020**, *717*, 11–19.

16. Kulaya, K.; Sujittra, R.; Pakpoom, R. Sensitivity of different physics schemes using WRF model in Typhoon Damrey (2017) over the Indochina region. *J. Phys.: Conf. Ser.* **2021**, *2145*, 012046.

17. Hunt, B.R.; Kostelich, E.; Szunyogh, I. Efficient data assimilation for spatiotemporal chaos: a local ensemble transforms Kalman filter. *Physica D*. **2005**, *230*, 112–126.

18. https://www2.mmm.ucar.edu/wrf/OnLineTutorial/compilation_tutorial.php.

19. http://homepages.see.leeds.ac.uk/~lecrrb/wrf/aRWUsersGuide.pdf.

20. Wilks, D.S. Statistical Methods in the Atmospheric Sciences, Ithaca New York. **1997**, *59*, 255.